ISTITUTO NAZIONALE DI FISICA NUCLEARE

Sezione di Roma II

INFN/TC-93/16
13 Settembre 1993

M.Ferrario, S.Kulinski, M.Minestrini, S.Tazzari:

MAGNETIC BOTTLE CONFIGURATION TO COAT 1.3 GHz COPPER CAVITIES WITH A Nb SPUTTERED FILM

Submitted to Nucl. Instr. & Meth. in Phys. Res.

Servizio Documentazione
dei Laboratori Nazionali di Frascati

INFN – Istituto Nazionale di Fisica Nucleare
Sezione di Roma II

INFN/TC-93/16
13 Settembre 1993

MAGNETIC BOTTLE CONFIGURATION TO COAT 1.3 GHz COPPER CAVITIES WITH A Nb SPUTTERED FILM

M.Ferrario*, S.Kulinski*, M.Minestrini*, S.Tazzari+

* INFN, LNF, P.O. Box 13, 00044 Frascati, Italy

+ University Tor Vergata and INFN Sez.Roma II, Via della Ricerca Scientifica 1, 00133 Roma, Italy

Abstract

An experimental setup to study the deposition of Nb film on TESLA type copper cavity is under commissioning. The discharge stabilizing magnetic field, in a magnetic bottle configuration, is obtained using coils external to the cavity rather than internal as used for larger cavities. A brief review of the sputtering techniques for SC RF cavities, the dynamics of charged particles in a magnetic bottle and the sputtering test setup are described.

I. SPUTTERING PROCESS: TECHNIQUE EVOLUTION FOR SUPERCONDUCTING ACCELERATING CAVITIES

Sputtering is a well known and useful technique for coating copper RF cavities with superconducting thin films. In the process, bombarding the surface of the cathode with ions (normally Argon ions accelerated by a static electric field) of sufficient energy (at least 30 eV), results in the ejection of cathode material in vapor form that deposits on the cavity walls forming a thin film [1].

The rather high energy of the incident ions ensures good adhesion of the film to the cavity copper walls even at rather low substrate temperatures; the cavity - that acts as substrate, anode and vacuum enclosure all at the same time - is thus prevented from deforming and, furthermore, its inside can be evacuated to sufficiently low pressure.

The simplest ions source to produce sputtering is based on the well known process of glow discharge between two electrodes in low pressure gas [2]; the discharge parameters characterizing the sputtering process are thus the gas pressure and the applied voltage or, equivalently, the ion density in the plasma, determining the discharge current, and the ion energy.

Since the probability of gas ionization and therefore the number of ions present in the discharge n_i, and the sputtering rate, are directly proportional to the gas pressure, there is a lower pressure

limit, depending on the distance between the electrodes, below which the sputtering rate becomes too low; on the other hand, the ion current and the deposition rate can be increased by increasing the pressure, up to the point when the mean free path of sputtered atoms becomes so short that the probability that they can reach the substrate and produce the film starts to decrease.

Furthermore, for the discharge to be self-sustaining, the energy of ions hitting the cathode, determined by the applied voltage, has to be high enough to extract secondary electrons and, in addition, each secondary electron must produce enough ions to release at least one new electron at the cathode.

The simplest configuration (diode), with just an electric field applied between a cathode and the copper substrate acting as anode, has a number of problems connected with the fact that the pressure for the discharge to become self sustained and the discharge current are both relatively high. This results in film contamination due to impurities coming from the pumping system (unavoidable at high working pressure) and from degassing of the chamber wall heated by the discharge, and in mechanical complexity of the cathode because of the cavity geometry [3], [4].

It is therefore instead desirable to keep the gas pressure and the wall temperature low while maintaining a high sputtering rate, i.e. a high average ion density in the gas.

To keep the sputtering rate constant as the gas pressure is decreased, one has to increase the ionization efficiency of free electrons by restraining the electron active path in the gas to the vicinity of the cathode - superimposing a perpendicular magnetic field onto the electric one - so as to give the electron a good chance to travel over a sizable fraction of its ionization mean free path before hitting the anode. This leads to the so-called magnetron sputtering configuration.

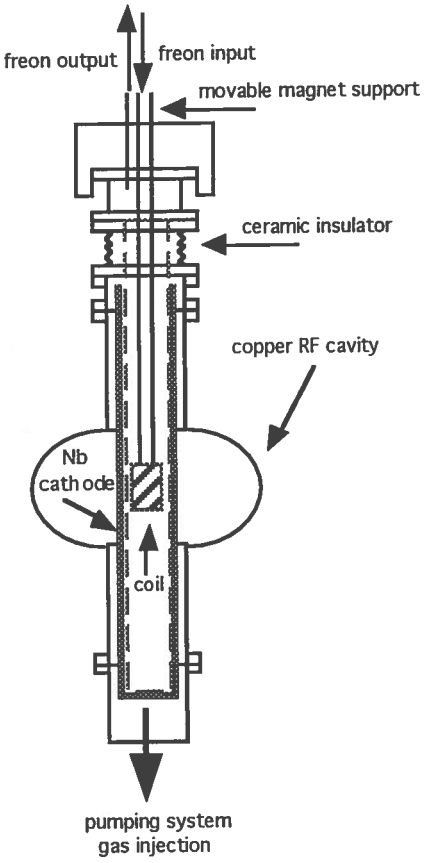

Figure 1. CERN magnetron sputtering scheme

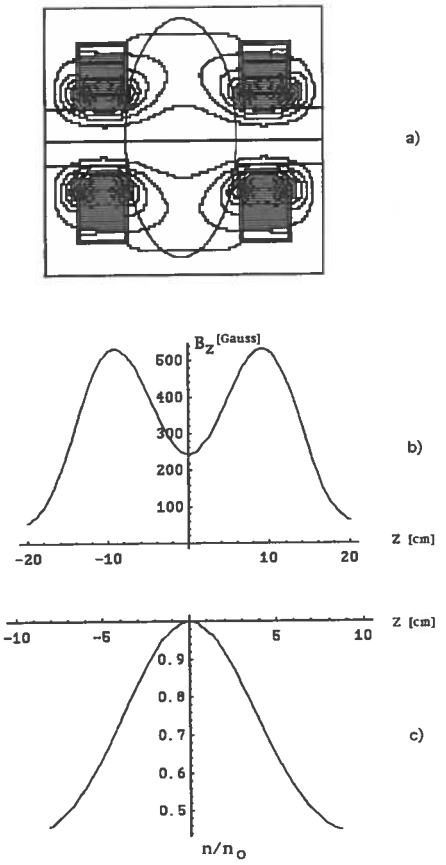

Figure 2.
a) Magnetic mirror field lines
b) Longitudinal magnetic field intensity on cathode surface
c) Normalized longitudinal plasma density

Magnetron sputtering to coat accelerating cavities with superconducting film was developed at CERN for 500 MHz cavities (Fig. 1), and is at present used in industry to coat 350 MHz copper cavities for LEP with Nb films [5]: the magnetic field is produced by a coil placed inside the cylindrical cathode and displaced in steps along the cavity axis to achieve a uniform coating.

While it is relatively easy to scale the technique up to larger cavities, scaling it down is more difficult unless small permanent magnets are used instead of a coil, making it however rather cumbersome to adjust the field shape and intensity to optimize the discharge parameters.

Because our setup is designed to coat 1.3 GHz cavities for TESLA that are 3 times smaller than the CERN ones, external coils placed on the outside of the cavity cut-off pipes (Fig.2a) and producing a magnetic mirror field configuration have been adopted, so as to preserve full control over the field shape and intensity. The magnetic mirror arrangement is well known from plasma physics [6]; the name refers to the fact that charged particles spiraling around a static magnetic field line will be reflected by a region of stronger field, because of the adiabatic constant of motion $\mu = mv_{\perp}^2 / 2B$.

II. MIRROR DESIGN

The magnetic bottle is created by two coils, placed on the outside of the cavity to be sputtered, along its axis, in correspondence with the cut-off tubes; they are surrounded by a dismountable 4 mm thick soft iron shield. The shield shape shown in Fig. 3 has been computed using a Poisson code to give a field minimum of about 200 Gauss at the center of the system and a mirror ratio (B_{max}/B_{min}) of about 2. The optimization of the shield configuration is obviously constrained by boundary conditions, such as cavity flange diameters and cavity length. Note that: in varying the diameter of the inner discs we can change the mirror ratio; adding a cylinder with diameter as the inner solenoid diameter the field peak can be shifted closer to the cavity center.

It allows to adjust the mirror ratio in the range 1 ÷ 3. This ratio is a measure of the trapping efficiency of the bottle. In fact charged particles are subject to an axial restoring force $F_z = -(dU(z)/dz)$, where $U(z) = \mu B(z)$ is a potential well proportional to the magnetic field strength, and are reflected if the condition $(v_{\perp} / v) \geq \sqrt{(B_{min} / B_{max})}$ holds; else, they are lost axially.

The nominal magnetic field of our setup is presented in Fig.2b. It should trap electrons and ions close to the midpoint of the cathode. The longitudinal charge density distribution is given approximately by $n(z)/n_0 = e^{-\frac{U(z)-U_{min}}{KT}}$ and is shown in Fig.2c for the case $(v_{\perp} / v) = 1/\sqrt{2}$.

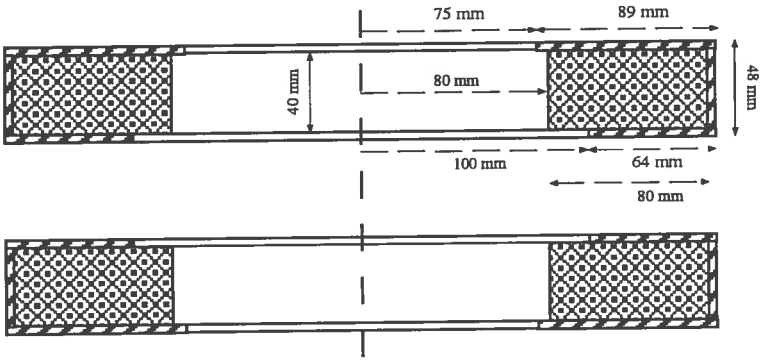

Figure 3. Coils cross section

The operating current density in the coils is estimated to be ≈5-8 Amp/mm^2, and the corresponding dissipated power is ≈(400-1000)W; water cooling is therefore provided.

III. SPUTTERING SETUP

The sputtering setup, assembled in a clean room (class 1000) at the University of Roma-Tor Vergata, is schematically shown in Fig. 4. It can accommodate different stainless steel TESLA type cavities (Fig. 5) on the inner walls of which, along the whole cavity profile, copper and sapphire samples can be fastened to allow studying the characteristics of the film over a wide portion of the surface. The Nb film is to be characterized by its RRR (Residual Resistivity Ratio) and T_c, and using Auger, SEM (Scanning Electron Microscope) and X rays analysis. Langmuir probes are provided to study the characteristics of the plasma.

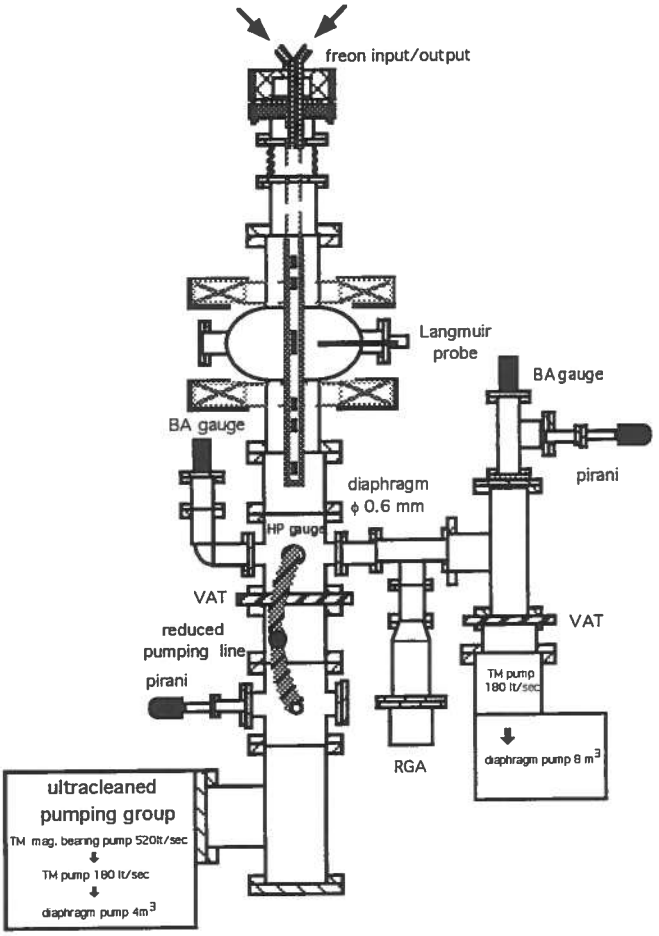

Figure 4. Sputtering system scheme

The system is evacuated by an ultraclean pumping group consisting of a 4 m^3/h diaphragm pump for the primary vacuum and two cascaded 180 l/sec and 520 l/sec turbomolecular pumps one of which on magnetic bearings. A very good compression ratio for hydrogen, good ultimate pressure ($\sim 10^{-10}$ mbar) and total absence of hydrocarbons is obtained.

The system is equipped with a residual gas analyzer (RGA) to study the ultimate pressure gas composition, and to monitor the percentage of gas produced during sputtering, notably hydrogen, that damages the film structure if it exceeds a certain threshold. To use the RGA while sputtering, in a relatively high operating pressure ($\sim 10^{-3}$ mbar), differential pumping is provided: the RGA communicates with the cavity through a 0.6 mm diaphragm and it is equipped with another pumping system that produces a 3 order of magnitude pressure drop through the diaphragm.

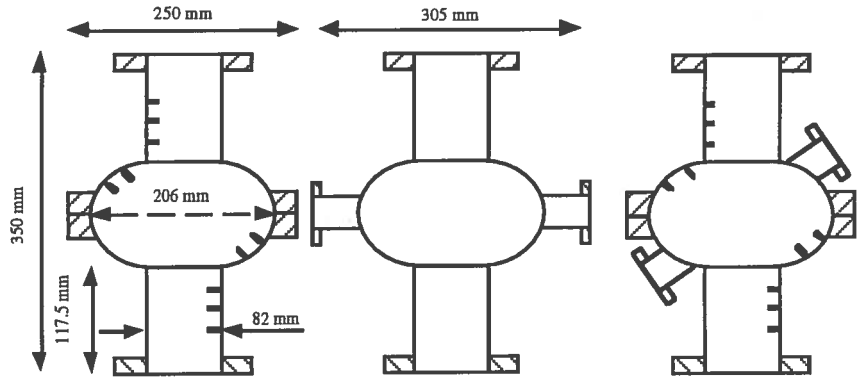

Figure 5. Stainless steel cavities

The cathode consists of a vacuum tight stainless steel tube (17 mm inner diameter) surrounded by a niobium liner (20/24 mm inner/outer diameters). The liner is a high purity Nb tube (RRR value better than 100) without welds. The stainless steel tube is also equipped with an inner support to hold and center 7 SamCo permanent magnets (small cylinders 8 mm diameter 16 mm long) cooled by a liquid freon circuit sized to handle about 2 KW of power. Preliminary tests to optimize discharge parameters will be carried out both with permanent magnets and with the magnetic bottle field configuration.

In order to better understand the discharge behavior and the actual sputtering mechanism, we have developed an approximate model and a numerical code the results of which are briefly described in the following

IV. EVALUATION OF THE PLASMA PARAMETERS

The number of Argon ions hitting the cathode and their energy depend on parameters of the plasma in the discharge such as ion and electron density and energy, Larmor radius, plasma Debye length, etc.: in the following we estimate the order of magnitude of the main plasma parameters within the range of discharge parameter typically found to give good results on existing sputtering setups, namely: pressure of the working gas $P \approx 10^{-4} \div 10^{-2}$ mbar, corresponding to densities $n \approx 3\ 10^{12} \div 3\ 10^{14}\ cm^{-3}$, applied voltage V≈ 500÷1000 V, magnetic field B≈200÷1000 Gauss.

The degree of ionization, n_i/n, can be rather easily estimated if one neglects the secondary electrons created by impinging ions and assumes that the cathode current is due to ions only (the number of secondary electrons is normally ≈ 10 times lower than that of ions).

The circulating current is then given by $I = q\, n_i\, v_i\, S_c$ where q is the ion charge, n_i the ion density, v_i the ion velocity and S_c the active surface of the cathode, and the ion density is given by equation

$$n_i = \frac{I}{q\, v_i\, S_c}. \qquad (4.1)$$

Assuming $S_c \approx 15 cm^2$, $v_i = 2.18 \times \sqrt{V} \times 10^5$ cm/sec and V= 400 Volt, one finally obtains:

$$n_i \approx 9.5 \cdot 10^{10}\ cm^{-3} \qquad (4.2)$$

Assuming further that $P \approx 10^{-3}$ mbar and therefore $n \approx 2.7 \times 10^{13}\ cm^{-3}$, the degree of ionization becomes

$$d_i = \frac{n_i}{n} \approx \frac{10^{11}}{2.7 \times 10^{13}} \approx 3.8 \times 10^{-3} \qquad (4.3)$$

Because the bulk of the plasma is neutral, one can set $n_e \approx n_i \approx 10^{11} cm^{-3}$; it is also reasonable to assume that the electron temperature (energy) is of the order of the ionization potential of Ar, namely $V_i \approx 15$ eV. One can therefore estimate the Debye length for the plasma λ_D, given by

$$\lambda_D[cm] = \sqrt{\frac{KT_e\varepsilon_o}{ne^2}} = 7.43\times10^2 T^{1/2}[eV] n_e^{-1/2}\left[cm^{-3}\right] \qquad (4.4)$$

For $T_e \approx 10$ eV and $n_e \approx 10^{11}$ cm^{-3}, one obtains $\lambda_D \approx 0.75 \times 10^{-2}$ cm.

Therefore, because the main potential drop in the plasma, in our case corresponding to the cathode drop, occurs over approximately one Debye length, one can assume that in this very thin sheet no collisions occur; all ions created in the plasma and reaching the cathode can thus be assumed to have at least an energy corresponding to the cathode voltage drop, or about 0.75÷0.80 of the total potential difference. The ion Larmor radius, given by $r_{Li} \approx 145\sqrt{A \cdot V} / B$, where A is the ion mass in atomic units, is consequently large: for Argon, with A~40 and an ion energy certainly higher than 100 eV, the radius for B=200 G is larger than ≈ 45 cm.

The electron Larmor radius is small but still considerably larger than the Debye length, so that electrons created at the cathode surface by impinging ions and also gaining about the same amount of energy as ions, can enter the bulk of the plasma and become the primary source of ionization. In fact, the electron Larmor radius is given by $r_{Le} = 3.4\sqrt{V} / B$, with V in Volts and B in Gauss, so that, taking $V = KT_e \approx 10$eV and B=200 G, one obtains : $r_{Le} \approx 5.3 \times 10^{-2}$ cm.

V. ELECTRON AND ION MOTION - TRAJECTORIES

To compute all discharge parameters one should self-consistently resolve the system containing field and transport equations and the boundary conditions. However, to understand the physics, a simplified model describing the motion of a single particle in known electromagnetic fields can be used effectively: it is briefly discussed below. For more detail, trajectory calculations have been performed numerically.

The simplified model is applicable as long as the collision frequency between particles is much smaller than the characteristic frequency of motion, or, in our case, of the cyclotron frequency ω_c ; i.e. one should have $(\omega_c / 2\pi)\cdot\tau_{coll} >> 1$, where $\tau_{coll} = 1/f_{coll}$ is the collision time.

Ions are easily seen to satisfy the above condition for the validity of the approximation since their Larmor radius is usually greater than the cathode-anode spacing so that, independently of where they are created, they move directly to the cathode. In the case of electrons it is shown in Appendix A that, in our setup, the condition is also usually satisfied.

As concerns electrons, an important characteristic of motion is that the electron Larmor radii, r_L, are much smaller than the distance over which the magnetic field changes considerably, i.e.

$$\alpha = r_L\left|\frac{gradB}{B}\right| \cong r_L\left|\frac{\Delta B}{\Delta r \cdot B}\right| << 1 \qquad (5.1)$$

In fact, in our setup, for B=200 Gauss and an electron energy ~10 eV, $\Delta B/B$ ~1 over Δr~5 cm and $r_L \sim 5.3\times10^{-2}$ cm, so that $\alpha \approx 10^{-3} << 1$.

When the above condition is fulfilled one is actually faced with motion in an adiabatically changing magnetic field so that the appropriate adiabatic constants such as the earlier mentioned $\mu = mv_\perp^2 / 2B$ can be used and furthermore, to find the shape of one electron orbit, one can safely assume that the magnetic field is constant.

The trajectory of an electron in a radial electric field, approximated by that, $E = K(r_1, r_2)/r$, of a cylindrical capacitor, superimposed on a constant axial magnetic field B_o is computed, including

collisions, in Appendix B. It is found that, on average, a collision causes the electron trajectory to be displaced radially by an amount r_{LD}, given by (eq.B.8)

$$r_{LD} = -\frac{E}{B_o \omega_L} . \qquad (5.2)$$

making it slowly drift towards the anode. With our parameters: B~200 G, ω_L~ 1.76×10^9 s^{-1}, an applied voltage V≈100V, and equivalent capacitor radii r_1~1.2 cm, r_2~10 cm, r_{LD} varies in the range $\approx 1.1 \times 10^{-2} \div \approx 1.3 \times 10^{-3}$. Taking it to be of order 6×10^{-3}, one estimates that to cover the distance between the center of the discharge and the anode an average electron should undergo ≈900 collisions, or else that to travel to ≈1 cm away from the cathode, a distance corresponding to an energy gain of ≈ 10 eV, it should undergo ≈160 collisions. Due to these frequent collisions the velocity distribution of electrons will be close to the truncated Maxwellian because of escape cone losses.

To analyze trajectories more precisely, a simple simulation code has been written that solves the equations of motion in axially symmetric, superimposed electric and magnetic fields. The code allows for the magnetic field to be a function of the longitudinal coordinate, z, and simulates collisions between particles. Some results of calculation are presented in Figs. 6 ÷ 10.

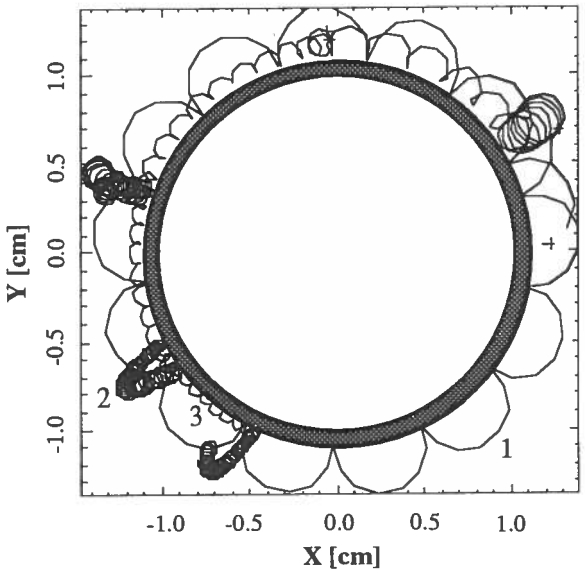

Figure 6. Simulated transverse electron trajectory with random collision (+)

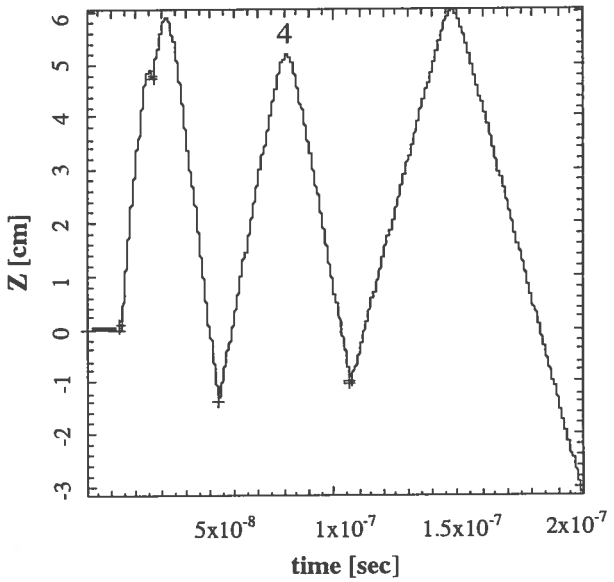

Figure 7. Longitudinal electron displacement including the effect of random collision (+)

Note that (see Fig. 6), unless a collision occurs, the electron path in the transverse plane (x,y) is always linked to the same magnetic field equipotential surface: an electron originating from the cathode experiences an intense electric field and starts to move in a cycloidal orbit around the cathode because of the $\mathbf{E} \times \mathbf{B}$ drift effect (orbit 1). As it experiences a collision, because collisions usually occur in the main plasma bulk where the electric field is weak, its orbit will become almost circular with a radius r_L depending on the initial transverse momentum (orbit 2). Furthermore, an electron with longitudinal component of the velocity, moves towards the stronger magnetic field end regions; its orbit is therefore brought nearer to the cathode and, if it enters the cathode-drop region, it restarts on a cycloidal path (orbit 3). In the longitudinal direction (z) (Fig 7) the electron is reflected by the mirror (orbit 4) when $(v_\perp / v) > 1/\sqrt{2}$. While the main drift is in the azimuthal direction, collisions do produce radial and axial drifts also (see Fig 8 and Fig. 9), in agreement with the predictions of the simplified model.

Argon ions can also undergo collisions, particularly with neutral atoms, before reaching the cathode. It can be shown that, for $P \geq 10^{-3}$ mbar, an ion starting from the center plasma region will on

average experience at least one collision before reaching the cathode. In fact, assuming that ions are created in the bulk of the plasma, at a distance from the cathode $\Delta R=R_{av}-R_c\approx$ (6-1.2) cm $\approx$ 5 cm and that their average energy gain is $\approx$ 100 eV, corresponding to the voltage drop in the main body of plasma, they will have an average velocity of $\approx 2\text{x}10^6$ cm/s; the average transit time to the cathode will thus be ≈ 2 μs and the average time in between e. g. elastic collisions $\tau_c[\text{sec}] = 1/n\langle\sigma v\rangle_{\text{elastic}} \approx \frac{3.4\cdot 10^{-9}}{P_{[\text{mbar}]}}$ sec thus giving at least one collision whenever $P \geq 10^{-3}$ mbar, q.o.d.

As concerns electron axial motion the presence of an appropriate magnetic mirror is essential. One can easily show that were they not present, electrons with axial velocity components would escape along the magnetic field lines in a time t_ℓ of the order 0.2 μsec: in fact, in each collision (e. g. with neutrals), an electron will on average acquire an axial velocity component after a time $\tau_{coll}=1/n\sigma v$. Taking $n=2.7\text{x}10^{13}$, $s=0.5\text{x}10^{-5}$ cm^2, $v=6\text{x}10^7$ cm/sec (corresponding to an energy of $\approx$ 1 eV), one finds $\tau_{coll}=1.3\text{x}10^{-7}$ sec and assuming L≈10 cm, one finds the quoted result.

Argon experiencing a collision before reaching the cathode will also acquiring an axial velocity and thus become capable of escape.

The energy variation of energetic electrons created at the cathode under the effects of random collisions is shown in the simulation of Fig. 10 An electron born on the cathode surface (see also Fig. 8) immediately gains the energy corresponding to the full 500 eV voltage drop and then starts to lose it because of ionizing collisions. After about 40 collisions its energy is damped to below the ionizing threshold. At such low energy it then starts to gain energy back, until another ionizing collision occurs.

For completeness, one should also mention that the confinement effect is actually somewhat reinforced by the fact (ambipolar diffusion) that because of their higher mobility, electrons tend to escape faster than ions, so that the boundary layer of plasma becomes positively charged making the axial diffusion of electrons more difficult.

Finally, the charge-exchange process $A^+ + B \rightarrow A + B^+$, with B an initially neutral atom and in which a neutral atom that immediately

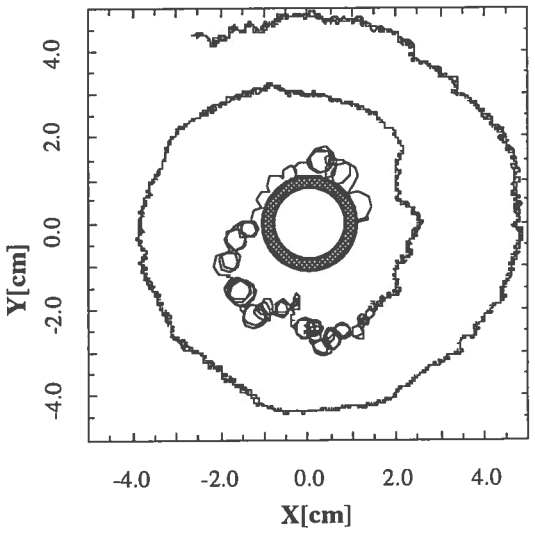

Fig.8. Electron trajectory on transverse plane

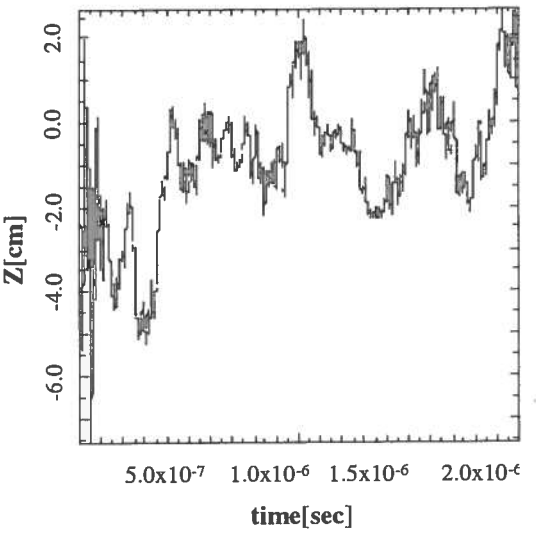

Fig. 9. Electron trajectory along the axis

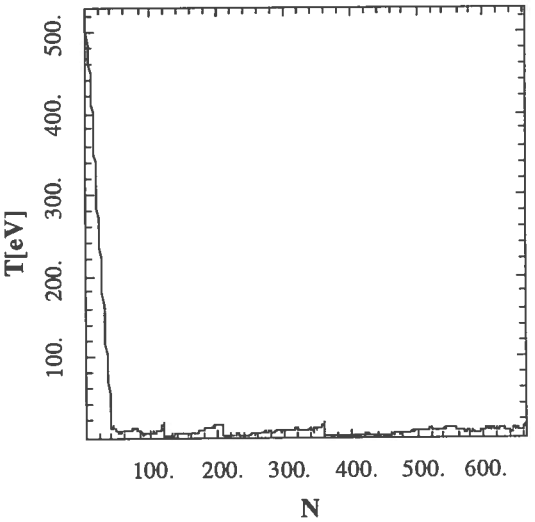

Fig. 10. Electron temperature versus number of collisions

escapes from the plasma and a slow ion are created, does also play a role in the sputtering discharge: charge exchange collisions will in fact tend to lower the sputtering rate because escaping neutrals striking the cathode, do not on average have enough energy to efficiently extract Nb atoms.

Note that the cross-section for charge transfer collisions is [11] $\approx (5\div6)\times10^{-15}$ cm^2 at an incident ion energy of 10 eV and about $(3\div5)\times10^{-15}$ cm^2 at 100 eV, and is thus comparable, in this energy range, to the elastic scattering cross-section.

In conclusion, from all above considerations one can see why the system operating pressure should be kept well below $\approx 10^{-3}$ mbar and why a proper magnetic mirror configuration must be implemented for proper functioning of the device.

APPENDIX A

To show that the condition $(\omega_c/2\pi)\cdot\tau_{coll} >> 1$ is usually fulfilled in our experiment, in particular for electrons, we note that the collision time is given by $\tau_{coll} = 1/n\langle\sigma v\rangle$ where $\langle\sigma v\rangle$ is the product $\sigma(v)*v$ averaged over the particle velocity distribution and $\sigma(v)$ is the collision cross section.

For electrons, there are two main processes contributing to $\langle\sigma v\rangle$: inelastic e-e collisions at low energy (low temperature) and elastic scattering on ions at high energy. Typically, the electron elastic scattering cross-section on Argon, σ_{el} , peaks at around (5÷10)eV reaching $\approx 2.5\times10^{-15}$ cm^2, while in the neighborhood of 100 eV the ionization cross section, σ_{ion}, is ~3×10^{-16} cm^2 [7].

At low energy, the characteristic collision time can be written [9]

$$\tau_c \approx \frac{14\cdot A^{1/2}\cdot 10^6\cdot T^{3/2}}{n\cdot Z^4 \ln\Lambda} \qquad (A.1)$$

where A is the mass of particle measured in atomic units, T the temperature in eV, n the particle density in cm^{-3}, Z the number of charges carried by an ion and ln Λ is a number of the order of 10 so that condition $f_c\ \tau_{coll} >> 1$ becomes:

$$\omega_{ce}\tau_{ce} = \frac{5.85\cdot 10^{12}\cdot T_e^{3/2}\cdot B}{n\cdot Z^4 \ln\Lambda} > 2\pi \qquad (A.2)$$

Taking $n_e \sim n_i \sim 10^{11}$ cm^{-3}, B~200 Gauss, lnΛ~5 it is seen that the lowest electron energy for which our model still holds is $T_{e\,min} \approx 2\times10^{-2}$ eV.

Now, there exist at least two groups of electrons in the sputtering discharge: the energetic electrons created at the cathode surface by impinging ions and the low energy electrons created by ionization inside the main plasma body. The former have an energy corresponding to the potential drop across the Debye length (usually more than 100 eV) and for them the condition $\omega_c\tau_{coll} >> 2\pi$ is certainly fulfilled. Furthermore, the measured temperature of electrons in the main bulk of a plasma is of the order of few eV so that also they make at least few cyclotron periods. The only possible exception comes in the case of very low energy electrons created by ionization in the main plasma body: these will however become maxwellized already after one collision, so that their contribution can be effectively neglected.

In the case of elastic collisions we have $\sigma_{el} \sim 2.5\times10^{-15}$ [8] ; assuming $n\sim3\times10^{13}$ (P~10^{-3} mbar)a velocity corresponding to energy of 100 eV and B=200 Gauss we get $\omega_{ce}\tau_{ce}\sim80$.

Finally, because the cross-sections for other collisions (ionization, excitation,..) are all much smaller than the two mentioned ones, we can conclude that in our plasma particles travel through many cyclotron orbits before colliding, and that the single particle model is therefore justified.

APPENDIX B

To analyze the motion of an electron in a radial electric field superimposed to a constant axial magnetic field, we write the Lagrangian L of a particle in the cylindrical coordinates :

$$L = \frac{m}{2}\left(v_r^2 + v_\varphi^2 + v_z^2\right) + qv \bullet A - q\phi \qquad (B.1)$$

where m is the mass, q the charge of a particle, r_2 is the anode radius and r_1 is close to the cathode radius and

$$\mathbf{A} = i_\varphi A_\varphi \ , \quad A_\varphi = B_0 \frac{r}{2} \ , \quad \phi(r) = V \frac{\ln(r/r_1)}{\ln(r_2/r_1)} \ .$$

Since the Lagrangian depends only on the radius r and the fields are static there are three constants of motion: the momenta p_z and p_φ and the total energy. Using these three constants one can find the trajectory of a particle in the form of quadratures [10] . For the radial motion one finds

$$\left(\frac{dr}{dt}\right)^2 = v_{ro}^2 + v_{\varphi o}^2 + r^2\left[\omega_L + \left(\frac{r_o}{r}\right)^2\left(\frac{d\varphi_o}{dt} - \omega_L\right)\right]^2 + 2\left(\frac{q}{m}\right)V\frac{\ln(r_o/r_1)}{\ln(r_2/r_1)} \ , \qquad (B.2)$$

where ω_L= -0.5(q/m), ω_L is the Larmor frequency and the subscript "o" denotes the value of a given quantity at time $t_0 = 0$. The equation can be simplified introducing a new variable $u = \ln(r_0/r)$ and noting that in our case $|u| << 1$. Expanding in powers of u and taking the terms up to u^2 we get

$$\left(\frac{dr}{dt}\right)^2 = R(u) = -au^2 + bu + c = -a(u_M - u)(u - u_m) \qquad (B.3)$$

with

$$a = 2r_o^2\left[\omega_L^2 + (\dot{\varphi}_o - \omega_L)^2\right] \ \text{and} \ \ b = -2r_o^2\left[(\dot{\varphi}_o - \omega_L)^2 - \omega_L^2 + \frac{q}{m}\frac{E_o}{r_o}\right] \qquad (B.4)$$

and where

$$c = v_{ro}^2 \quad , \quad E_o = \frac{V}{r_o \ln(r_2/r_1)} \ , \qquad (B.5)$$

$$u_M = \frac{b}{2a} + \sqrt{\left(\frac{b}{2a}\right)^2 + \frac{c}{a}} = \ln\frac{r_o}{r_m} \ ; \ u_m = \frac{b}{2a} - \sqrt{\left(\frac{b}{2a}\right)^2 + \frac{c}{a}} = \ln\frac{r_o}{r_M} \ .$$

The radial motion is periodic and r changes between minimum $r_m = r_o e^{-u_M}$ and maximum $r_M = r_o e^{-u_m}$. The period T of the motion and the changes Δz and $\Delta\varphi$ of z and φ during a period can be found to be [10]

$$T = \frac{2\pi}{\sqrt{a}} e^{-(b/2a)} \cdot I_0\left(\frac{u_M - u_m}{2}\right) \ ; \ \Delta z = v_{zo} T \ ; \ \Delta\varphi = \omega_L + (\dot{\varphi}_o - \omega_L)\, e^{b/a} \qquad (B.6)$$

where I_0 (x) is the modified Bessel function of order 0.

We can now give the complete description of a particle motion in between collisions. As mentioned above the radial motion is periodic and a particle oscillates between r_m and r_M with the period T. There is an average azimuthal speed $v_\varphi = r_o\langle\dot{\varphi}\rangle$ given by

$$v_\varphi = r_o\frac{\Delta\varphi}{\Delta T} = r_o\left[\omega_L + (\dot{\varphi}_o - \omega_L)e^{-b/a}\right]$$

Because usually $|\dot{\varphi}_o| << |\omega_L|$, it can be shown that

$$\frac{b}{a} \approx -\frac{E_o}{\omega_L B_o r_o}\left(1 + \frac{\dot{\varphi}_o}{\omega_L}\right) + \frac{\dot{\varphi}_o}{\omega_L} << 1, \ \text{so that} \ \ v_\varphi \approx -\frac{E_o}{B_o}\left[1 - \left(\frac{\dot{\varphi}_o}{\omega_L}\right)^2\right] \approx v_D \qquad (B.7)$$

where $v_D = -E_o/B_o$ is the known drift velocity in crossed **E, B** fields.

If there were no magnetic mirrors the axial motion would be monotonic with a constant velocity v_{zo}: the mirrors force most of the electrons to oscillate in between them, thus preventing them from escaping.

Finally, knowing r_m and r_M we can find the average displacement $\langle \Delta r \rangle$ of an electron from the initial position r_o . Setting

$$\Delta r = \frac{1}{2}(r_M + r_m - 2r_o) \approx -r_o \frac{b}{a} \approx \frac{v_D}{\omega_L}\left(1 + \frac{\dot{\varphi}_o}{\omega_L}\right) - r_o \frac{\dot{\varphi}_o}{\omega_L}$$

and because after each collision $\dot{\varphi}_o$ can be either positive or negative but the average $\langle \dot{\varphi}_o \rangle$ taken over all electrons is zero, $\langle \Delta r \rangle$ is given by

$$\langle \Delta r \rangle = \frac{v_D}{\omega_L} = r_{LD} \qquad \text{(B.8)}$$

showing that it is equal to the "Larmor radius" corresponding to the drift velocity v_D.

Acknowledgments

The authors gladly acknowledge the help given by W.De Masi in designing and characterizing the solenoids and for the work done in the development of tracking code.

References

[1] J.A.Thornton, A.S.Penfold, Thin film processes, edited by J.L.Vossen, Academic Press, New York (1978).
[2] J.L. Delcroix, An Introduction to the Theory of Ionized Gases, Wiley, New York (1960)
[3] C.Benvenuti, N.Circelli, M.Hauer, W.Weingarten, IEEE Trans. Magn. MAG-21 153 (1985).
[4] C.Benvenuti, N.Circelli, M.Hauer, Appl. Phys. Lett. 45, 5 (1984).
[5] C.Benvenuti, D.Bloess, E.Chiaveri, N.Hilleret, M.Minestrini, W.Weingarten, Proc. 3rd Workshop on RF Superconductivity, ANL-PHI-88-1, vol.2.
[6] T.K. Fowler, Mirror Theory, in Fusion , vol. 1 part A, edited by E. Teller, Academic Press (1981)
[7] K.Wasa, S.Hayakawa, Transactions on Parts, Materials and Packing, pmp-3, n.3 (1967)
[8] J.B.Hasted, Physics of atomic collisions, London Butherworths (1964)
[9] L. Spitzer. Physics of fully ionized gases, Interscience, New York (1956)
[10] S.Kulinski, Plasma physics, vol. 8, Pergamon Press (1966)
S. Kulinski, Plasma physics, vol. 10, Pergamon Press (1968)
[11] D.R.Bakes (editor), Atomic and molecular processes, Academic Press., New York and London (1962)